

## Article

# Mitigating Harmful Effects of Climate Warming on Ceiling Paintings by Ceiling Insulation: An Evaluation Using Timed IR Imaging and Numeric Modelling

Günther Kain <sup>1,2,3,\*</sup>, Friedrich Idam <sup>2,3</sup>, Alfons Huber <sup>4</sup>, Martin Mudri <sup>5</sup>, Alexander Petutschnigg <sup>1</sup> and Markus Goldsteiner <sup>6</sup>

<sup>1</sup> Department for Forest Products Technology and Timber Construction, Salzburg University of Applied Sciences, Markt 136a, 5431 Kuchl, Austria; alexander.petutschnigg@fh-salzburg.ac.at

<sup>2</sup> Department for Wood Restoration Technology, Higher Technical College Hallstatt, Lahnstraße 69, 4830 Hallstatt, Austria; idam@gmx.at

<sup>3</sup> ICOMOS Austria, Karlsplatz 13, 1040 Vienna, Austria

<sup>4</sup> Independent Researcher, Herbeckstraße 62/8, 1180 Vienna, Austria; alfons-huber@aon.at

<sup>5</sup> Mudri Measuring Technology, Schanzelgasse 20/3, 8010 Graz, Austria; martin.mudri@zt-mudri.at

<sup>6</sup> Bundestheater-Holding GmbH, Goethegasse 1, 1010 Vienna, Austria; markus.goldsteiner@bundestheater.at

\* Correspondence: gkain.lba@fh-salzburg.ac.at

**Abstract:** Due to climate change, ceiling paintings in many historic buildings are subjected to increasingly high short-term temperature change, resulting in high thermal tension caused by the construction assembly. This article focuses on the combined use of timed IR imaging and numeric modelling to evaluate insulation measures on the upper side of a ceiling to reduce thermal tensions in the painting layers, overheating in summer as well as cooling down in winter. As a model room, the southern splendour stair hall in the Burgtheater Vienna was chosen. Famous ceiling paintings created from 1886 to 1888 by Gustav Klimt and his brother Ernst Klimt can be found on this ceiling. The results show that timed IR imaging is an adequate tool to study the transient thermal behaviour of ceiling paintings which are not accessible to standard sensor measurements. Moreover, it could be shown that the presented measurement technique is well suited to validate a numeric model. The latter was applied to evaluate the potential insulation on the top of the ceiling. It was shown that cooling loads and energy loss in the room underneath can be reduced and most importantly the thermal stress in painting layers is reduced. The findings are relevant as, due to global warming, the current situation in many buildings is worsening. Considering the great intangible cultural value of many ceiling paintings, the application of the presented evaluation strategy for building physical boundaries on a ceiling with paintings seems to be appropriate.

**Keywords:** ceiling insulation; infrared thermography; secco painting; FE modelling; thermal tensions; overheating protection; simple smart buildings



**Citation:** Kain, G.; Idam, F.; Huber, A.; Mudri, M.; Petutschnigg, A.; Goldsteiner, M. Mitigating Harmful Effects of Climate Warming on Ceiling Paintings by Ceiling Insulation: An Evaluation Using Timed IR Imaging and Numeric Modelling. *Sustainability* **2022**, *14*, 308. <https://doi.org/10.3390/su14010308>

Academic Editor: Asterios Bakolas

Received: 29 November 2021

Accepted: 22 December 2021

Published: 28 December 2021

**Publisher's Note:** MDPI stays neutral with regard to jurisdictional claims in published maps and institutional affiliations.



**Copyright:** © 2021 by the authors. Licensee MDPI, Basel, Switzerland. This article is an open access article distributed under the terms and conditions of the Creative Commons Attribution (CC BY) license (<https://creativecommons.org/licenses/by/4.0/>).

## 1. Introduction

The average temperature in the city centre of Vienna has risen by more than 2 °C within the last 30 years and is expected to rise even more until the end of this century [1,2]. An expert interview amongst cultural heritage experts has shown that mitigation of climate change also requires measures in the cultural built heritage sector, which is a complex multivariate task [3]. They agree on the fact that cultural heritage has to be adapted in order to mitigate harmful effects of climate change on the building heritage [4] and to ensure visitor comfort [5]. Rising temperatures display a risk for the cultural heritage because of both thermal stress in construction elements and inappropriate alterations to the historic construction when introducing engineering solutions [6].

Aiming to ensure visitor comfort, in many historic buildings, cooling strategies are considered. In cultural heritage, a compromise between visitor comfort and preservation of

artwork regarding climate conditions has to be found—a challenge that can be addressed by using numerical simulation tools [7]. A study in the Uffizi Gallery, Florence, has shown that the microclimate created with HVAC systems can be disadvantageous to art objects because temperature and relative humidity are not in balance with the ones of the building structures. The latter very often is characterised by thick and massive walls in traditional buildings. Interestingly, during days where the HVAC system was out of operation, the best conservational conditions for paintings were observed [8]. A similar study was published in 2008 by the facility management of the Germanic National Museum, Nuremberg [9].

Apart from classical air conditioning systems, it was shown that traditional buildings, such as the Burgtheater Vienna, can be cooled by applying a combination of controlled ventilation with a minimized cooling degree, shadowing and insulation of selected construction elements [5]. The Burgtheater is equipped with an air-well system originating from construction time, a system which was shown to be suitable for modern climate control in the Neue Burg, Vienna [10]. A key for developing effective cooling strategies for traditional buildings is the consideration of the high thermal mass of massive construction elements [11].

A study on a temple in Bangkok, Thailand, has revealed that ceiling insulation, low absorption roofs and attic ventilation are a means to lower peak indoor temperatures in old buildings. Passive cooling strategies rather than HVAC systems are used in Buddhist temples because of religious constraints [11]. Extreme temperature conditions can harm art objects and can even lead to a substantial change of pigments in paintings [12], which was confirmed to a minor extent by the cracks on the Klimt paintings in the Burgtheater [13]. Ceiling insulation attenuates the temperature peaks in a construction element by increasing its thermal mass and lowering the heat flow rate through it. This physical fact is relevant for light constructions, such as the ceiling of the splendour stair hall in the Burgtheater Vienna. It was shown in this context that the commonly used calculation of U-values does not precisely reflect the ceiling's thermal behaviour because the benefits of a construction's thermal mass are not taken into consideration [14]. It was shown that numerical models can be used to study the effects of thermal insulation on ceilings with complex cross sections [15]. Multi-sensor in situ measurements are an effective measure to test the validity of models [16,17].

Infrared thermography is a non-invasive method in building research to visualize hidden structures or construction elements, using differences in thermal conductivity when there is a sufficiently large temperature difference between inside and outside. Another approach is to use differences in heat storage capacity when unheated buildings are investigated [18]. Stimulated infrared thermography can be applied in painting restoration to detect painting structures. The painting that shall be analysed is excited with a flux of photons, and the surface temperature is increased, depending on the material's thermal characteristics, resulting in a temperature variation [19]. Timed infrared imaging analysis was used to study decay mechanisms related to moisture presence in St. Eldrad's chapel near Turin, Italy [20], or to detect delaminations in fresco plaster [21].

The Burgtheater Vienna was built at the end of the 19th century and is both one of the most important and the second oldest straight theatre in Europe. It was planned by Gottfried Semper and Carl Hasenauer and is equipped with, for those times, advanced building equipment such as an air ventilation tunnel, developed by Carl Böhm and Eduard Meter.

The building consists of the central theatre and two spacious stair halls with a barrel vault (Figure 1). Its construction is a clasps construction with brickwork fillings. A similar vault construction can be found in the Museum of Natural History in Vienna, which was erected at the same time as the Burgtheater [22]. The metal construction likely consists of wrought iron because the use of Martin steel for such constructions was obligatory not before 1894 in the Danube Monarchy [23].

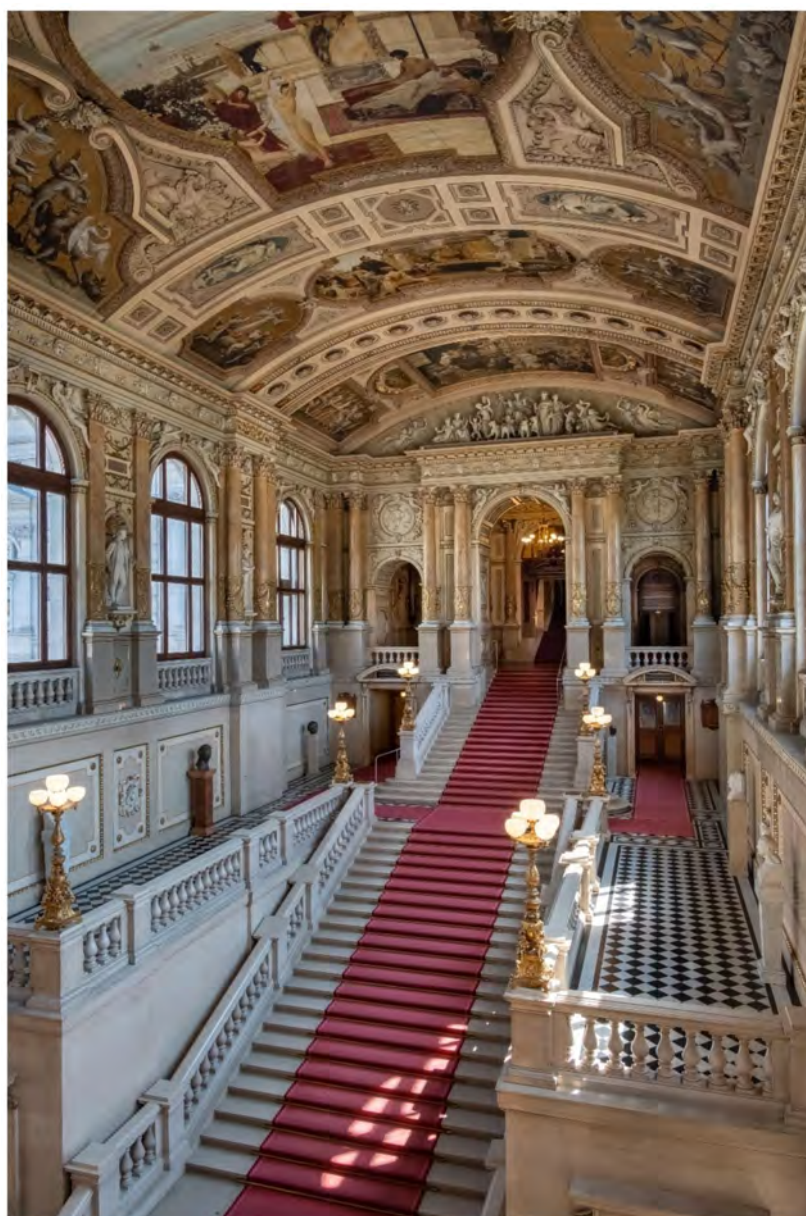


**Figure 1.** Splendour stair hall of the Burgtheater with ceiling paintings created by Gustav Klimt [24].

The arched ribs, carrying the segment barrel vault, are mounted with a distance of 82 cm in the plane of the vault. The ribs are curved and have a T- or rectangular cross section with a height of 12 cm and a width of 2.5 cm. These ribs made of wrought iron have their support in the lateral walls of the staircase and hang on five purlin-like lattice girders made from wrought iron running in the length direction of the stair hall. Between these ribs, there are brick elements with poured-in clasps hanging in the ribs, the latter with a distance of 10 cm on average. The bricks are covered with mortar with a thickness of 1 to 4 cm on their upper side. The mortar layer is levelled with the iron ribs, and the clasps carrying the brick filling are visible from the upper side [19]. Contrary to the vault in the Museum of Natural History, where the vault is filled with a Hourdis-Creux system [17], solid bricks were used in the Burgtheater. This was shown by a local opening of the plaster in the attic [25]. Towards the lower side, there is most likely a wooden lathing with a metal lattice plaster base attached.

Considering the time of origin, the plaster on the bottom of the vault is highly probably lime plaster with a thickness of 15 mm. In the area of the ceiling ornaments, the plaster is significantly thicker.

The final painting layer of the paintings at the border, which were decorated by Karl Josef Geiger, was attached using the marouflage technique. Smooth and slightly pasty oil painting on canvas with Panama binding was attached to the ceiling using probably white lead. The central paintings on the ceiling of the staircase were painted by Gustav Klimt using the oil-bound secco technique [13,26].

A recent expert opinion from 2020 focusing on the conservation status of the paintings showed that they are in good condition, despite minor dust deposits and small local hollow areas. Nevertheless, alongside the iron ribs, the paintings show little cracks [13], probably due to the high thermal loads caused by the quick warming and cooling of the iron elements [27].

## 2. Research Aim

In many historical buildings with ceiling paintings such as the stair hall of the Burgtheater Vienna, the heat input via the ceiling must be reduced to minimize thermal stress on the valuable ceiling paintings. The winter energy loss and the heat input in summer via the ceiling should also be reduced for reasons of costs and visitor comfort. Between 1982 and 2019, the daily mean temperature in the city centre of Vienna rose by 0.1 °C throughout the year [2]. This development emphasizes the need to address the issue. This study focused on combined long-term measurements of thermal boundaries and transient IR imaging of a ceiling with paintings. The results were used to validate a finite element (FE) model, which is used to evaluate whether insulation on the ceiling's upper side is suitable to lower short-term temperature variations on its bottom side.

## 3. Materials and Methods

### 3.1. In Situ Measurements

Measurements of the ceiling of the southern staircase of the Burgtheater Vienna were conducted between 18 February and 13 August 2020 (171 days, Figure 2). From March 10, the warm-air heating system of the stair hall was out of operation due to the closure of the theatre because of the COVID-19 restrictions. This is a fortunate occasion for the current research project because the languid building structure could be studied without heating interference.

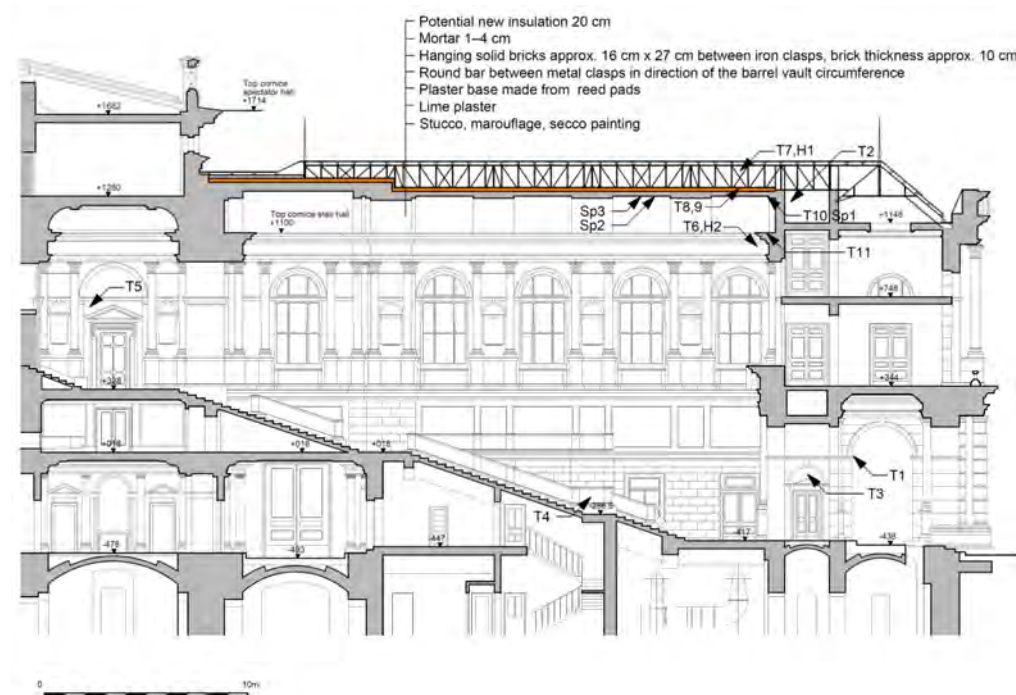


Figure 2. Section through the southern splendour stair hall with position of the sensors [28].

During this period, the air temperature, air humidity and surface temperatures on the ceiling's upper side were logged. Additionally, the air temperature and the air humidity were measured at various positions in the stair hall. Surface temperatures were evaluated at the lower side of ceiling on the southern narrow side of the stair hall, above the ceiling cornice. Figure 2 and Table 1 provide an overview of sensor positions and measured parameters. Measurements were logged in a time interval of 30 min (time interval suggested in a similar study [29]). The surface temperatures were logged near the southern archive stair hall of the head building which are influenced by a thick plaster layer of the ornaments and interactions with the southern massive transverse wall of the archive stair hall. Due to the theatre use and conservational reasons, it was not possible to place sensors in the central field of the paintings. To gain information on the central ceiling, the area of the temperature sensors and the central ceiling, high-resolution thermography with a time interval of 15 min was recorded between May 30 and April 4. These were used to gain information about the planar temperature distribution on the ceiling and to parameterise the thermal model. Thermography allows for an estimation of the transient thermal behaviour of the ceiling construction by a comparison of the different thermal storage capacities of the ceiling sectors. A FLIR T640 IR camera system with a 45° objective was used. The emissivity of the outer ceiling layer was estimated with a value of 0.92, and an object distance of 17 m and an atmospheric temperature of 20 °C were considered. The reflected measuring temperature was set to 22 °C and the relative air humidity to 55%.

**Table 1.** Position and type of sensors.

Position of the Sensor	Sensor ID	Measuring Device (Sensor)
Exterior temperature	T1	Testo 174 T
Archive stair hall attic	T2	Testo 174 T
Archive stair hall ground floor	T3	Testo 174 T
Stair hall intermediate landing	T4	Testo 174 T
Stair hall after staircase	T5	Testo 174 T
30 cm below ceiling cornice	T6	Almemo 5690
Stair hall attic	T7	Almemo 2590
Attic surface mortar	T8	Almemo 2590
Attic surface iron clasps	T9	Almemo 2590
Surface painting	T10	Almemo 5690
Ceiling cornice east corner	T11	Almemo 5690
Air humidity attic	H1	Testo 174 H
Air humidity stair hall	H2	Almemo 5690
IR spot ceiling cornice	Sp1	FLIR T640
IR spot iron ribs	Sp2	FLIR T640
IR spot field	Sp3	FLIR T640

### 3.2. FE Model

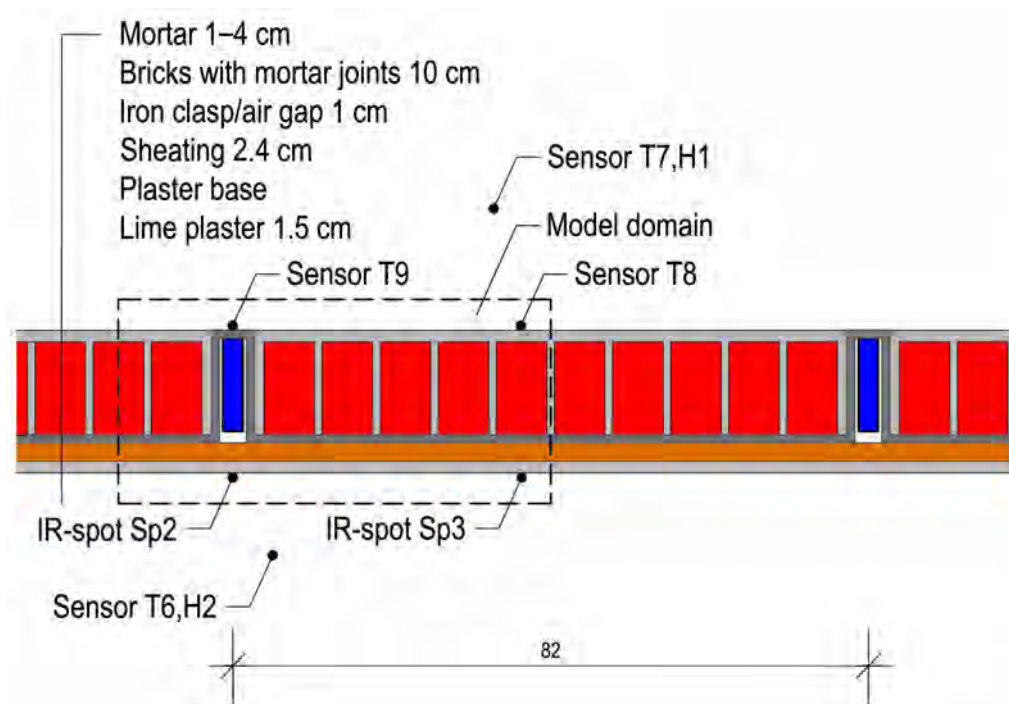
In order to evaluate the implications of potential ceiling insulation, the ceiling of the splendour stair hall was modelled using the Software Delphin 5.8.1 [30] in a two-dimensional consideration. A section, crosswise to a steel rib, with a length of 50 cm including an iron rib, was considered in the model. The FE model was applied first with the given construction to evaluate its validity by comparing modelled values with measured values, and second, a potential insulation layer with 20 cm of blow-in insulation was applied. Cellulose insulation was chosen because due to static reasons and the complex geometry of the attic (lattice girders as purlins), a light and easy-to-build-in insulation would have to be used [25]. Material properties were considered as shown in Table 2 and documented by Bauklimatik Dresden Software GmbH [30] and Sontag et al. [31].

**Table 2.** Estimated ceiling construction of the splendour stair hall.

Position of the Sensor	Thickness (cm)	Density (kg/m <sup>3</sup> )	Spec. Heat Capacity (J/kgK)	Thermal Conductivity (W/mK)	$\mu$ - Value (-)
Cellulose insulation	20	55	2544	0.048	2
Lime plaster	1	2100	1000	2.1	9
Iron rib	11.5	7800	470	47	200,000
Solid brick	11.5	1600	950	0.78	9
Air layer	1.5	1.3	1050	0.9	1
Lathing/air (mix layer)	2.5	200	1245	0.14	5
Lime plaster	1.5	1500	800	0.4	9

The air temperature and humidity in the attic and the stair hall were imposed on the model as boundary conditions using the measured values.

The model domain ( $50 \times 38$  cm, Figure 3) was discretized using variable discretization (smaller elements at material boundaries) with a minimum element width of 1 mm, which resulted in 2709 rectangular elements considered in the model.

**Figure 3.** Cross section through ceiling construction with position of the sensors.

The surface temperature at the ceiling's lower side in the field (corresponding to Sp3) and below an iron rib (corresponding to Sp2) was modelled considering an average of 10 finite elements in line each.

## 4. Results and Discussion

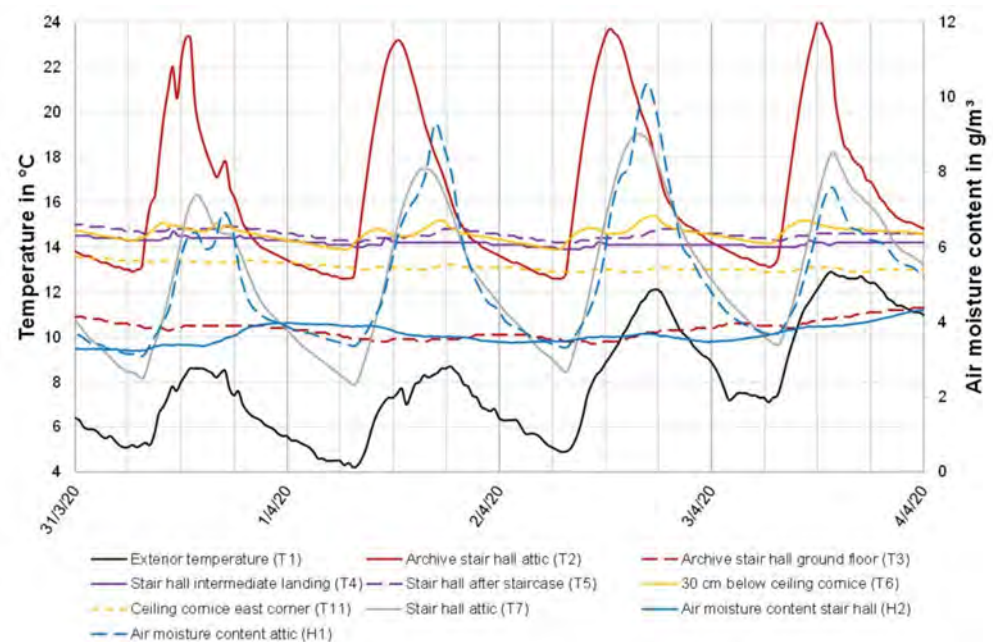
### 4.1. Microclimatic Analysis of the Stair Hall

During the measuring time, an average outside temperature in the entrance area of the southern stair hall (T1, in the shadow) of  $17.2$  °C (SD  $5.9$  °C) was recorded. On March 23, a minimum of  $2.7$  °C and on July 28 a maximum of  $37.8$  °C were measured (Table 3).

**Table 3.** Descriptive statistics for measured values, time period 18 February and 13 August 2020.

Position of the Sensor		Average	SD	Minimum	Maximum
Exterior temperature (T1)	°C	17.2	5.9	2.7	37.8
Archive staircase attic (T2)	°C	24.9	6.1	12.0	43.5
Archive staircase ground floor (T3)	°C	17.9	4.1	9.0	33.2
Stair hall intermediate landing (T4)	°C	20.7	3.2	13.9	32.4
Stair hall after staircase (T5)	°C	21.2	3.5	14.2	32.7
30 cm below ceiling cornice (T6)	°C	21.8	3.8	13.9	30.3
Stair hall attic (T7)	°C	21.5	6.4	7.9	37.7
Attic surface mortar (T8)	°C	20.9	5.7	8.7	34.1
Attic surface iron clasps (T9)	°C	21.0	5.5	9.4	33.3
Surface painting (T10)	°C	20.8	4.2	11.9	29.6
Ceiling cornice east corner (T11)	°C	20.8	4.2	12.6	30.10
Air humidity attic (H1)	%	48.1	6.7	30.8	74.4
Air humidity stair hall (H2)	%	41.0	8.7	22.0	61.0
Vapour pressure stair hall (H1)	Pa	1130	440	415	2179
Vapour pressure attic (H2)	Pa	1306	525	423	3577
Air moisture content attic (H1)	g/m <sup>3</sup>	9	4	3	26
Air moisture content stair hall (H2)	g/m <sup>3</sup>	8	3	3	16

In the attic of the stair hall (T7), the average temperature was 21.5 °C (SD 6.4 °C), 4.4 °C higher than the outside temperature. Whilst the latter reaches its maximum at 6 pm, the former has a daily maximum at around 4 pm due to the radiation input over the roof surface. Both outside and attic temperature is characterized by a sinusoidal 24-h course (Figures 4 and 5).

**Figure 4.** Temperature in the stair hall during cold period.

The air temperature during the measuring period at the upper end of the staircase of the lateral archive stair hall in the head building of the southern splendour stair hall (T2) accounted for 24.9 °C on average (standard deviation (SD) 6.1, minimum 12.0, maximum 43.5 °C). The temperature reached its maximum around 1 pm. This is caused by the high input of radiation energy through the above situated translucent smoke flap and the roof windows in the adjacent attic. The air temperature at the ground floor of the archive (T3) stair hall is constantly lower (Figure 4).

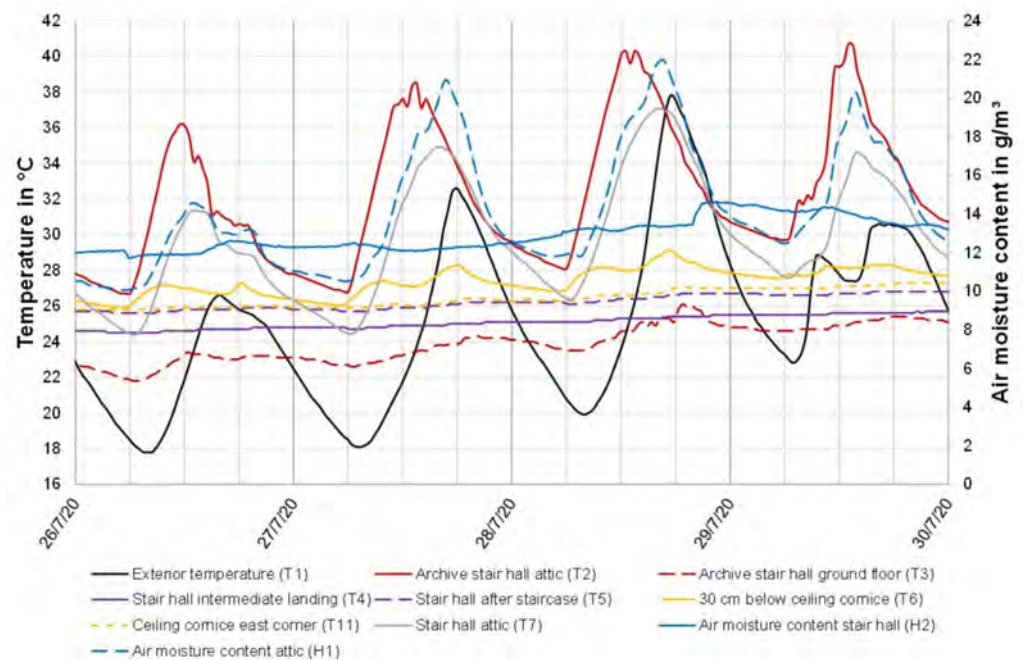


**Figure 5.** Temperature in the stair hall during hot period.

In the stair hall, the air temperature was measured 30 cm below the cornice near the ceiling (T6) and accounted for 21.8 °C on average (SD 3.8, minimum 13.9, maximum 30.3 °C). It is characterized by a bimodal course with a temporal maximum reached at approximately 9 am caused by the eastern radiation input and at 8 pm caused by the western radiation input through the large windows. This temperature course is reflected with increasing damping at the ceiling's lower side (T10) and in the eastern building corner (Figures 4 and 5). The temperature in the stair hall is 25% of the time higher than 25 °C which is out of the range for artwork conservation recommended by UNI 10829 [32]. The change of the outdoor temperature and the temperature in the stair hall attic is gradual during the measuring time, whilst the air temperature distribution inside the stair hall is bimodal indicating a distinct spring and summer climate [8].

The air temperature on the stair itself, on the intermediate landing (T4) and at the end of the stair (T5) is very constant. Daily peaks are strongly attenuated, and the temperature follows the multi-day temperature with an average of 20.7 and 21.2 °C, respectively.

Whilst the warm-air heating is out of operation, the vertical temperature gradients in the stair hall are low. Low gradients prevent air flow resulting in deposition of airborne particles and wall and ceiling soiling [33].

#### 4.2. Air Humidity

The air moisture content in the stair hall (H2) accounted for 8 g/m<sup>3</sup> on average (SD 3, minimum 3, maximum 16 g/m<sup>3</sup>) during the measurement time. In the attic above (H1), the average air moisture content was 8 g/m<sup>3</sup> (SD 4, minimum 4, maximum 26 g/m<sup>3</sup>). Very low humidity was measured in the midst of March 2020 (relative humidity in the stair hall as low as 22%) when unusually low exterior temperatures were recorded and the heating system was on. The air humidity develops parallel with the outside air temperature and the attic air temperature accordingly (Figures 4 and 5). This fact indicates a high air change rate in the attic. In contrast, the air moisture is very constant in the stair hall following the multi-day trend of the indoor temperature.

Humidity variations inside the stair hall would be even stronger with normal visitor numbers (restrictions due to the COVID-19 crisis). From a conservatory point of view, the short-term humidity variation should be low to avoid material tensions [6]. The standards for proper conservation of oil painting on dry plaster (10 °C < T < 24 °C;

50% < RH < 60%) [34,35] were exceeded temperature-wise 28% of the investigated time period, and the RH fell 80 % of the time below the optimum and did not exceed 60%. Short-term deviations of plus–minus 5% of the limits are acceptable [35], but in the current study, RH was constantly lower than 50% from the midst of February until the beginning of June. The excessive drops of RH due to heating in cold climates are highly problematic for artworks [36]. The low RH could be avoided by limited use of warm-air heating, a heating technology that is seen as problematic for all kinds of artwork conservation [36]. The high temperatures inside the stair hall could be reduced by shadowing systems of the large windows, an optimized ventilation strategy (using the existing air-well system [5]) and ceiling insulation, which is discussed in this paper. The choice of these measures is in accordance with a study on the optimization of Buddhist temples in Bangkok recommending similar cooling strategies [11].

#### 4.3. Water Vapour Diffusion

Water vapour diffusion processes in the ceiling construction of the stair hall are governed by the surrounding climate (air temperature and humidity) in the stair hall and the attic and by the ceiling construction. The water vapour pressure in the stair hall at the start of the measuring campaign was predominantly lower than the one in the attic, which is a result of the higher air humidity and temperature peaks in the attic (Figure 6). The same can be observed in summer, although less pronounced (Figure 7). Diffusion processes occur from the attic to the stair hall. As the diffusion proceeds towards the warm side, there is now risk of condensation. In the current study, the cold winter months were not investigated. With low temperatures in the attic and high air moisture humidity in the stair hall, there would be the risk of condensation in the construction of the ceiling [37]. Such climatic parameters should be addressed in further research.

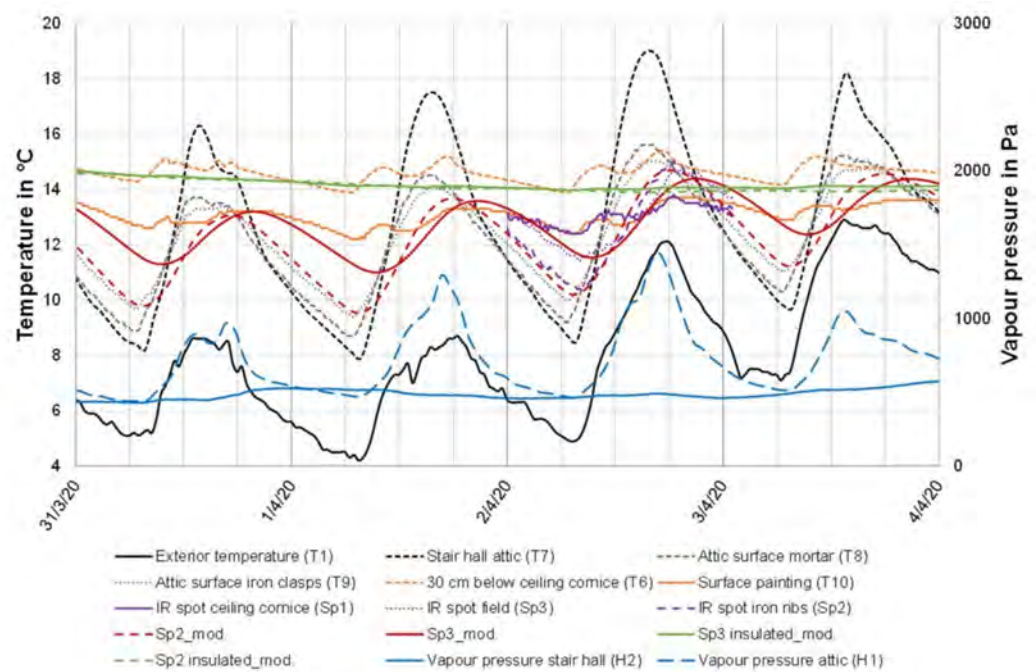
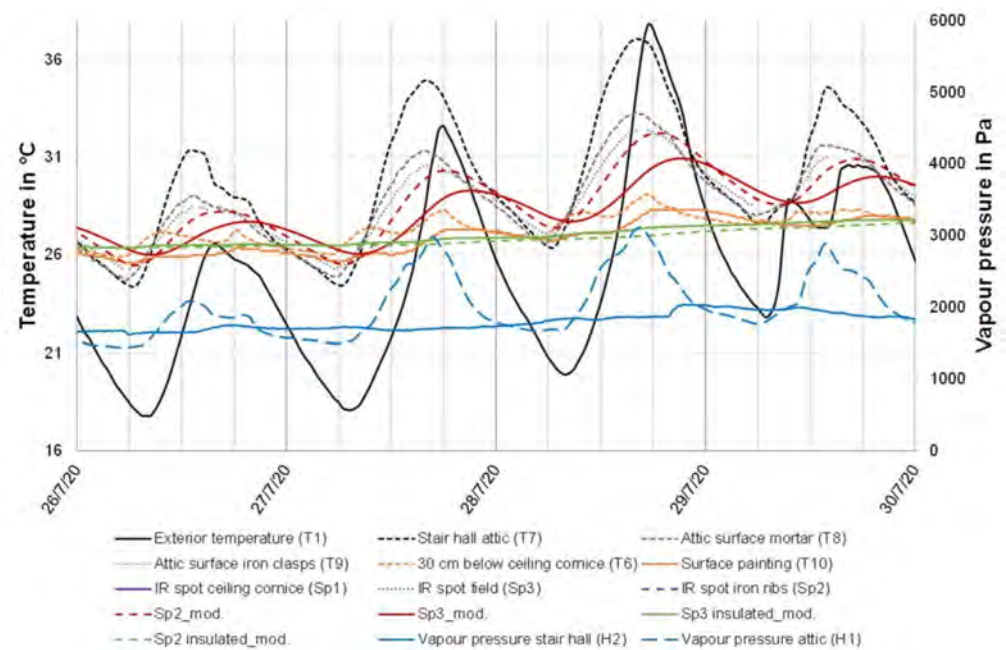


Figure 6. Temperature at the ceiling during cold period, including model results.



**Figure 7.** Temperatures at the ceiling during hot period, including model results.

#### 4.4. Surface Temperatures at the Ceiling

Focusing on surface temperatures, the one on the plaster surface on the upper side of the ceiling (T8) on average accounted for 20.9 °C (SD 5.7 °C) and follows the daily course of the air temperature in the attic, whereby the peaks are significantly attenuated (Figures 6 and 7). This results in a 0.6 °C lower average and a 0.7 °C lower SD. On the iron clasp standing out of the plaster layer (T9), the average surface temperature is insignificantly higher (average 21.0 °C, SD 5.5 °C) than the one on the plaster. Notably, the amplitude of the surface temperature on the iron clasps compared with the surface temperature of the field between the ribs is dampened, which is a result of the high thermal conductivity and specific heat storage capacity of the iron (Figures 6 and 7).

The temperature at the surface of the ceiling painting next to the transverse wall (T10) accounted for 20.8 °C on average (SD 4.2 °C) with a minimum of 11.9 and a maximum of 29.6 °C. Especially short-term temperature change is problematic for the conservation of paint layers due to thermal expansion and contraction. On July 28 (maximum of the outside temperature at 6 pm 37.6 °C), the surface temperature at the measuring point of the painting accounted for 27.7 °C at 6 am, 27.1 at 11 am, 28.3 °C and 27.7 °C at 6 am on the following day. The 24-h temperature range accounts for 1.3 °C. This range is even more pronounced around the steel ribs.

Analysing the IR data, good accordance between measured surface temperatures and temperatures derived from IR thermography could be observed. On average, the surface temperature gained by IR measurement of measuring point Sp1 deviated by 0.04 °C (SD 0.18 °C) from the surface temperature measured directly at point Sp1 (Figures 8 and 9). In areas where the fixation of sensors was not possible, thermography can be used to estimate surface temperatures. According to Figures 8 and 9, the thermal diffusivity of the construction alongside the iron ribs is significantly higher than in the field area in between, as the temperature span is much higher in the area mentioned first.

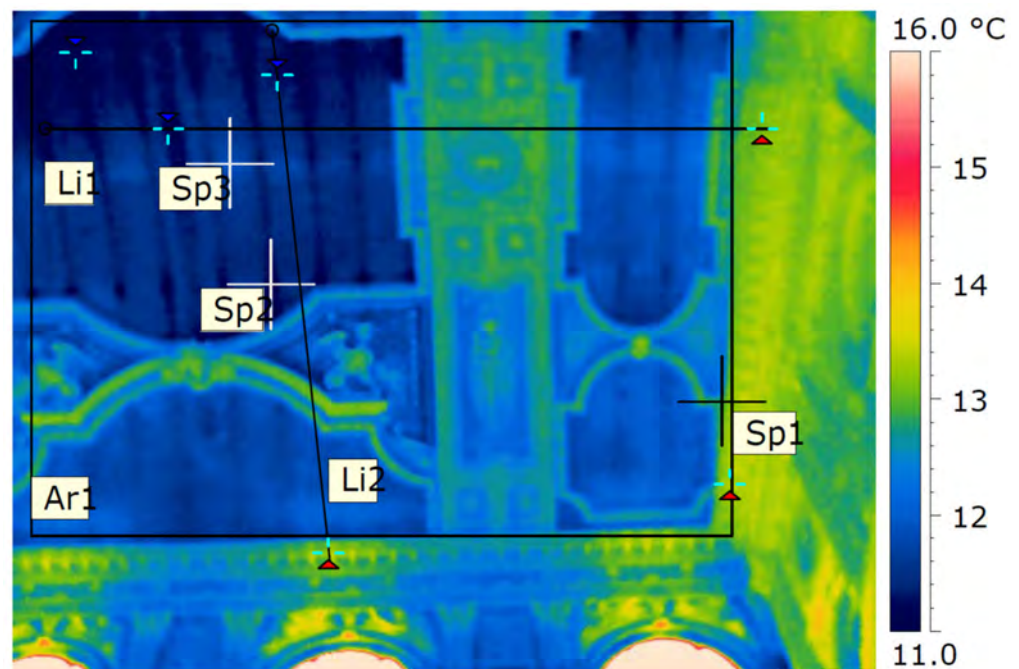


**Figure 8.** Thermography of the soffit on April 2, 9:45 am (see Supplementary Materials).

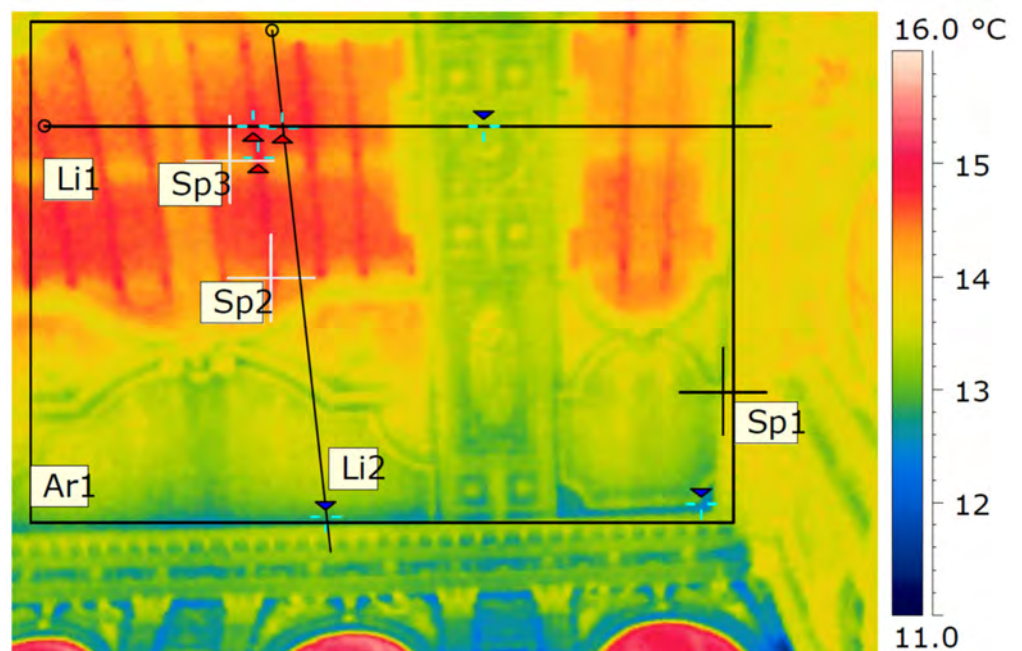


**Figure 9.** Thermography of the soffit on April 2, 5:30 pm (see Supplementary Materials).

#### 4.5. Results of the Numeric Model

The model for the temperature at the painting surface at the measuring points Sp2 and Sp3 captures the course of the real measured temperature quite well.

Slight deviations are probably caused by erroneous assumptions regarding the structures of the ceiling, which is a problem inherent to numeric models in building research [38]. Most likely the deviations occurred in the estimation of the thickness of the plaster layer at the top (as it is heterogeneous), the design of the lathing and the plaster thickness at the vault's underside. The physical properties of the materials were estimated according to Table 2 when implementing them in the model. The global problem setting seems to be well described by the model because it reflects the real course of temperatures quite well.

On average, the model underestimates the real measured surface temperature of the field (Sp3) by 0.04 (SD = 0.29) °C.

In the model, the application of a 20 cm thick cellulose insulation was evaluated. It would attenuate the temperature amplitude by 2.5 °C on hot days (Figure 7) which would reduce the thermal stress in the painting layers. Over the total measuring campaign, the daily temperature variations would be significantly reduced by the insulation (Figure 10). In the current state, on more than 50 days of the investigated 171 days, the daily temperature span at measuring point Sp2 exceeded 4 °C. The maximum span occurs thereby in a time span of approximately 12 h (Figure 10). In the case of the insulated ceiling, the maximum temperature span would be below 1 °C.

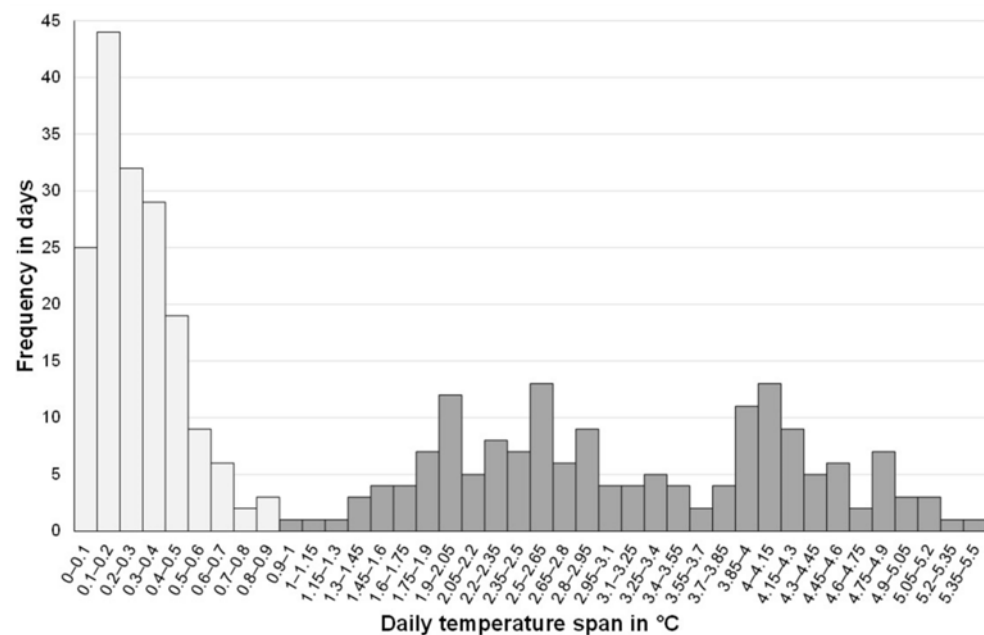


**Figure 10.** Daily temperature variations in the central ceiling field (measuring point Sp2).

The implications of the ceiling insulation shall be discussed exemplarily for 28 July (day 160 of the measuring campaign) with an exterior temperature maximum of 37.8 °C and a maximum temperature of 27.0 °C in the attic. The four days before July 28 were characterized by rising exterior temperatures as a lot of heat energy had been stored in the construction. On July 28, the surface temperature in the centre of the field (Sp3) accounted for 30.9 °C at 9 pm according to the model. Given the case that the ceiling was insulated with 20 cm cellulose flocs on its upper side, the temperature would be 27.5 °C at the specified position. In the area under the iron ribs, the temperature at the ceiling would be 32.2 °C at 6 pm or 27 °C, respectively, when insulated. The maximum value is reached earlier compared to the field because the thermal diffusivity is higher in this region. Figure 11 shows that the high temperatures at the upper side of the ceiling do not diffuse through the ceiling with ceiling insulation. Moreover, the insulation layer lowers the thermal bridge via the iron ribs, and hence, more homogeneous temperature conditions can be anticipated at the paint layers. The most important effect of the ceiling insulation is, apart from a reduction of the ceiling's U-value (reduction from 1.58 W/(m<sup>2</sup>K) to 0.19 W/(m<sup>2</sup>K) in the field between the ribs), an almost complete elimination of daily amplitudes of the temperature at the painting layer, which reduces the thermal stress significantly.

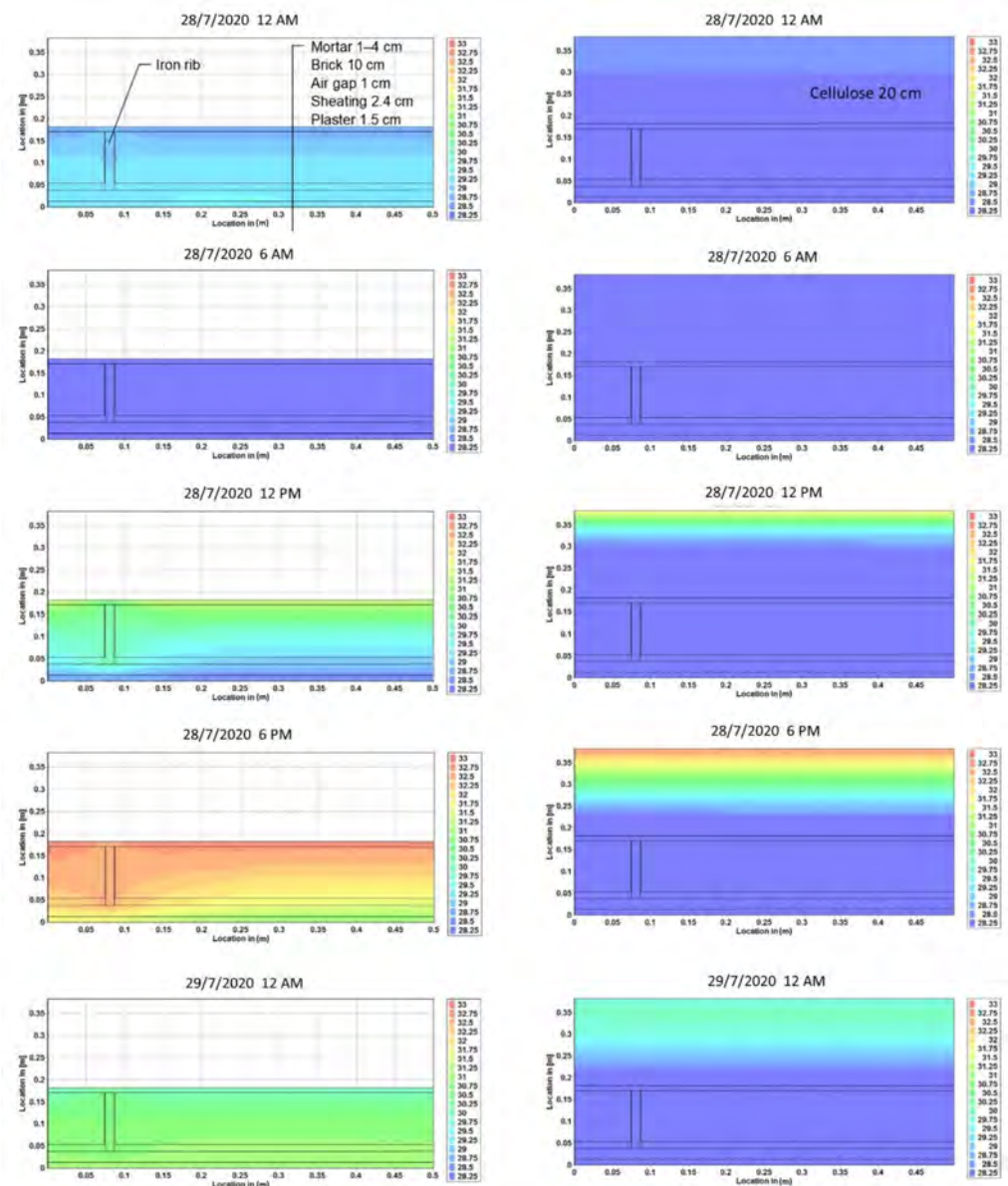


Figure 11. Finite element model of ceiling in the stair hall between July, 28, 12 am and July 29, 12 am (left column without insulation, right column with 20 cm cellulose insulation, time step 6 h).

## 5. Conclusions

The measurements carried out on the ceiling paintings in the southern splendour stair hall of the Burgtheater Vienna demonstrate that the temperature variation on the painting surface is high. The daily temperature variation was higher than 4 K for more than 50 days during summer 2020. This was especially pronounced below well-heat-conducting structure elements such as iron ribs. As the average temperature will be rising in Central Europe, the problem is likely to get worse in the future.

IR thermography proved to be well suited for the investigation of painting surface temperatures as it displayed very little deviation from contact surface measurements. This finding is of practical relevance because the erection of scaffolds is costly and sometimes impossible due to theatre operations.

Timed IR thermography was shown to be a means to visualize hidden structures and to understand the 2D transient thermal behaviour of a complex construction such as the clasps construction of the vault in the Burgtheater.

The FE model could be successfully applied to extend the findings of the IR measurements to a longer period. This seems to be an adequate approach because timed IR thermography is costly and time consuming in data evaluation. Nonetheless, the application of FE models in building research requires real measurements to parameterize and validate the model.

It was shown by a thermal FE model that an insulation layer on the upper side of a ceiling reduces the short-term temperature variation at the painting layer significantly. Moreover, it would reduce the heat energy loss in winter and the heat input from the attic in summer.

For the splendour hall of the Burgtheater, it was shown that the steam diffusion processes would be rather unproblematic because, in the investigated time period (February 18 until August 13), the vapour pressure in the attic was predominantly higher than in the stair hall, meaning that diffusion proceeds from the upper to the lower side, and due to the relatively high temperatures on the ceilings' bottom side, no condensation has to be considered. This might change during very cold periods and if humidity rises in the stair hall and should therefore be investigated in further research.

**Supplementary Materials:** The following are available online at <https://www.mdpi.com/article/10.3390/su14010308/s1>, Video S1: IR fast motion Burgtheater Vienna.

**Author Contributions:** Conceptualization, G.K., F.I. and A.H.; methodology, G.K., F.I. and A.H.; software, G.K.; validation, G.K., F.I., A.H., A.P. and M.G.; formal analysis, G.K., F.I., A.H. and M.G.; investigation, G.K., F.I., A.H. and M.M.; resources, G.K., M.M., A.P., and M.G.; data curation, G.K. and M.M.; writing—original draft preparation, G.K., F.I. and A.H.; writing—review and editing, G.K., F.I., A.H., A.P. and M.G.; visualization, G.K.; supervision, G.K., F.I., A.H. and M.G.; project administration, G.K., F.I., A.H. and M.G.; funding acquisition, G.K. and F.I. All authors have read and agreed to the published version of the manuscript.

**Funding:** This project was funded by Department 4 in Section IV of the Austrian Ministry for Art, Culture, Public Service and Sports and by ICOMOS Austria.

**Institutional Review Board Statement:** Not applicable.

**Informed Consent Statement:** Not applicable.

**Data Availability Statement:** Not applicable.

**Acknowledgments:** The authors are grateful for the financial and organizational support of Christian Kircher, managing director of the Bundestheater-Holding GmbH and Robert Beutler, commercial director of the Burgtheater, who thankfully provided critical input to the manuscript. Finally, they want to thank the employees of the building services department in the Burgtheater, namely Bernd Sailer and Martin Prerost, for their support when mounting and demounting the sensors and for the supply of technical equipment.

**Conflicts of Interest:** The authors declare no conflict of interest.

## References

1. Zentralanstalt für Meteorologie und Geodynamik. Klima Aktuell—Klimamonitoring—Tagesmitteltemperaturen Wien Hohe Warte. Available online: <https://www.zamg.ac.at/cms/de/klima/klima-aktuell/klimamonitoring/?param=t&period=period-ymd-2020-04-02&ref=3> (accessed on 3 April 2020).
2. Umweltbundesamt GmbH. Der Klimawandel in Wien. Available online: [https://data.ccca.ac.at/dataset/factsheet\\_der\\_klimawandel\\_in\\_wien-v01/resource/445ce4cf-7d12-464e-b9ec-0b10f65e1ca8](https://data.ccca.ac.at/dataset/factsheet_der_klimawandel_in_wien-v01/resource/445ce4cf-7d12-464e-b9ec-0b10f65e1ca8) (accessed on 5 April 2020).
3. Sesana, E.; Bertolin, C.; Gagnon, A.; Hughes, J. Mitigating Climate Change in the Cultural Built Heritage Sector. *Climate* **2019**, *7*, 90. [CrossRef]
4. Sesana, E.; Gagnon, A.; Bertolin, C.; Hughes, J. Adapting Cultural Heritage to Climate Change Risks: Perspectives of Cultural Heritage Experts in Europe. *Geosciences* **2018**, *8*, 305. [CrossRef]
5. Kain, G.; Idam, F.; Huber, A.; Goldsteiner, M. Luftbrunnenanlage des Burgtheaters Wien: Nachhaltige Klimatisierungsstrategien (Air well system of the Burgtheater Vienna: Sustainable cooling strategies). *Bauphysik* **2021**, *43*, 1–11. [CrossRef]
6. Sabbioni, X.; Cassar, M.; Brimblecombe, P.; Lefevre, R. *Vulnerability of Cultural Heritage to Climate Change: European and Mediterranean Major Hazards Agreement*; Council of Europe: Strasbourg, France, 2008.

7. Balocco, C. Daily natural heat convection in a historical hall. *J. Cult. Herit.* **2007**, *8*, 370–376. [[CrossRef](#)]
8. Camuffo, D.; Bernardi, A.; Sturaro, G.; Valentino, A. The microclimate inside the Pollaiuolo and Botticelli rooms in the Uffizi Gallery, Florence. *J. Cult. Herit.* **2002**, *3*, 155–161. [[CrossRef](#)]
9. Heydecke, F. Aus Alt mach Neu—Meine Klimaanlage macht nicht was ich will. *Beiträge Zur Erhalt. Von Kunst-Kult. VDR Fachz.* **2008**, *1*, 101–106.
10. Huber, A. Ökosystem Museum. Grundlagen zu Einem Konservatorischen Betriebskonzept für die Neue Burg in Wien. Ph.D. Thesis, Akademie der Bildenden Künste Wien, Wien, Austria, 2011.
11. Sreshthaputra, A.; Haberl, J.; Andrews, M. Improving building design and operation of a Thai Buddhist temple. *Energy Build.* **2004**, *36*, 481–494. [[CrossRef](#)]
12. Doménech-Carbó, M.T.; Edwards, H.G.; Doménech-Carbó, A.; del Hoyo-Meléndez, J.M.; de La Cruz-Cañizares, J. An authentication case study: Antonio Palomino versus Vicente Guillo paintings in the vaulted ceiling of the Sant Joan del Mercat church (Valencia, Spain). *J. Raman Spectrosc.* **2012**, *43*, 1250–1259. [[CrossRef](#)]
13. Koller, M. Untersuchung der Deckenbilder und Stuckrahmungen in der SO-Ecke der südlichen Feststiege des Burgtheaters. *Expert Opinion*. **2020**, unpublished.
14. Byrne, A.; Byrne, G.; Davies, A.; Robinson, A.J. Transient and quasi-steady thermal behaviour of a building envelope due to retrofitted cavity wall and ceiling insulation. *Energy Build.* **2013**, *61*, 356–365. [[CrossRef](#)]
15. Drobiec, L.; Wyczółkowski, R.; Kisiołek, A. Numerical Modelling of Thermal Insulation of Reinforced Concrete Ceilings with Complex Cross-Sections. *Appl. Sci.* **2020**, *10*, 2642. [[CrossRef](#)]
16. Kain, G.; Gschwandtner, F.; Idam, F. Der Wärmedurchgang bei Doppelfenstern—Konzept zur In-situ-Bewertung historischer Konstruktionen. *Bauphysik* **2017**, *39*, 144–147. [[CrossRef](#)]
17. Kain, G.; Idam, F.; Federspiel, F.; Réh, R.; Krišťák, L. Suitability of Wooden Shingles for Ventilated Roofs: An Evaluation of Ventilation Efficiency. *Appl. Sci.* **2020**, *10*, 6499. [[CrossRef](#)]
18. Mudri, M. Möglichkeiten und Grenzen der Thermografie. Bauforschung an historischen Gebäuden mittels Infrarot-Untersuchung. *Sachverständige* **2017**, *4*, 188–196.
19. Bodnar, J.L.; Candoré, J.C.; Nicolas, J.L.; Szatanik, G.; Detalle, V.; Vallet, J.M. Stimulated infrared thermography applied to help restoring mural paintings. *NDT E Int.* **2012**, *49*, 40–46. [[CrossRef](#)]
20. Cadelano, G.; Bison, P.; Bortolin, A.; Ferrarini, G.; Peron, F.; Girotto, M.; Volinia, M. Monitoring of historical frescoes by timed infrared imaging analysis. *Opto-Electron. Rev.* **2015**, *23*, 100–106. [[CrossRef](#)]
21. Grinzato, E.; Bison, P.; Marinetti, S.; Vavilov, V. Nondestructive evaluation of delaminations in fresco plaster using transient infrared thermography. *Res. Nondestruct. Eval.* **1994**, *5*, 257–274. [[CrossRef](#)]
22. Wehdorn, M. *Die Bautechnik der Wiener Ringstraße*; Steiner: Wiesbaden, Germany, 1979.
23. Stadler, G. Expert Opinion on the Construction of the Vault in the Burgtheater Vienna. **2020**, unpublished.
24. Heindl, K. Photography splendour stair hall Burgtheater Vienna, Vienna. unpublished.
25. Fritze, R. Deckenaufbau Burgtheater Decke Über Feststiege. *Expert Opinion* **2020**, unpublished.
26. Koller, M. Marouflagemalerei um 1900: Zur Restaurierung des Wiener Parlamentfrieses. *Restauro* **1996**, *102*, 406–409.
27. Arendt, C. The role of the architectural fabric in the preservation of wall painting. In Proceedings of the Conservation of Wall Paintings: Proceedings of a Symposium Organized by the Courtauld Institute of Art and the Getty Conservation Institute, London, UK, 13–16 July 1987.
28. Bundestheaterholding. Plans of the Burgtheater Vienna, Vienna. unpublished.
29. Merello, P.; García-Diego, F.-J.; Zarzo, M. Microclimate monitoring of Ariadne's house (Pompeii, Italy) for preventive conservation of fresco paintings. *Chem. Cent. J.* **2012**, *6*, 145. [[CrossRef](#)] [[PubMed](#)]
30. Bauklimatik Dresden Software GmbH. Delphin—Programm- und Modelldokumentation. Available online: [www.bauklimatik-dresden.de/delphin/documentation](http://www.bauklimatik-dresden.de/delphin/documentation) (accessed on 18 April 2020).
31. Sontag, L.; Nicolai, A.; Vogelsang, S. *Validierung der Solverimplementierung des Hygrothermischen Simulationsprogramms Delphin*; Technical Report; Technische Universität Dresden: Dresden, Germany, 2013.
32. UNI 10829. *Works of Art of Historical Importance—Ambient Conditions or the Conservation—Measurement and Analysis*; Uni: Rome, Italy, 1999.
33. Zarzo, M.; Fernández-Navajas, A.; García-Diego, F.-J. Long-term monitoring of fresco paintings in the cathedral of Valencia (Spain) through humidity and temperature sensors in various locations for preventive conservation. *Sensors* **2011**, *11*, 8685–8710. [[CrossRef](#)]
34. Erhard, D.; Mecklenburg, M. Relative Humidity re-examined, Preventive Conservation. *Prepr. IIC-Ott. Congr.* **1994**, 32–43.
35. Thompson, G. *The Museum Environment*, 2nd ed.; Routledge: London, UK, 2018.
36. Camuffo, D.; Pagan, E.; Rissanen, S.; Bratasz, L.; Kozłowski, R.; Camuffo, M.; Della Valle, A. An advanced church heating system favourable to artworks: A contribution to European standardisation. *J. Cult. Herit.* **2010**, *11*, 205–219. [[CrossRef](#)]
37. Bernardi, A.; Todorov, V.; Hiristova, J. Microclimatic analysis in St. Stephan's church, Nessebar, Bulgaria after interventions for the conservation of frescoes. *J. Cult. Herit.* **2000**, *1*, 281–286. [[CrossRef](#)]
38. Mundt-Petersen, S.O.; Harderup, L.-E. Predicting hygrothermal performance in cold roofs using a 1D transient heat and moisture calculation tool. *Build. Environ.* **2015**, *90*, 215–231. [[CrossRef](#)]